NATIONAL ADVISORY COMMITTEE FOR AERONAUTICS

TECHNICAL NOTE 4312

INTERNAL CHARACTERISTICS AND PERFORMANCE OF AN AERODYNAMICALLY CONTROLLED, VARIABLE-DISCHARGE CONVERGENT NOZZLE

By Jack G. McArdle

Lewis Flight Propulsion Laboratory
Cleveland, Ohio

Washington

July 1958

NATIONAL ADVISORY COMMITTEE FOR AERONAUTICS

TECHNICAL NOTE 4312

INTERNAL CHARACTERISTICS AND PERFORMANCE OF AN AERODYNAMICALLY CONTROLLED, VARIABLE-DISCHARGE CONVERGENT NOZZLE

By Jack G. McArdle

SUMMARY

The effective flow area of a convergent exhaust nozzle was reduced by injecting a high-pressure secondary jet into the nozzle near the exit. Analytical expressions relating the performance with significant design and operating variables were developed, and necessary experimental factors were evaluated by using a 4-inch-exit-diameter nozzle with unheated pressurized air discharged to the atmosphere. The effective flow area was reduced as much as 67 percent, while the ratio of actual thrust to the thrust attainable from primary and secondary isentropic expansion was 0.94 or better in nearly all cases. Some of the configurations, altered to operate as jet deflectors, produced significant values of side force but, at the same time, operated at reduced effective flow area.

INTRODUCTION

Modern turbojet engines often use variable-area primary exhaust nozzles to help keep thrust high and specific fuel consumption low under all operating conditions. Nozzle area usually is varied by mechanically adjusting the exit to the required size by means of interconnected leaves. However, the effective flow area of a fixed nozzle can be continuously varied over a wide range by suitably injecting a secondary jet into the nozzle. This method, which is equivalent to mechanical exit variation and could eliminate problems arising from weight, complexity, and actuator power, is reported to be in operational use in France (ref. 1).

An investigation of this method of varying the effective flow area of a convergent nozzle was conducted at the NACA Lewis laboratory. (Ref. 2 gives the results of an independent British investigation of this type device.) Analytical expressions relating the performance with significant operating and design variables were developed. The experimental coefficients required in these expressions were evaluated by using a 4-inch-exit-diameter nozzle with unheated pressurized air discharged to the

atmosphere. Primary- and secondary-pressure ratios ranged from 1.6 to 2.8 and from 2.0 to 7.7, respectively. The secondary jet was injected with no axial momentum through a continuous circumferential slot. For some tests the model was altered to operate as a jet deflector.

APPARATUS AND INSTRUMENTATION

Models

The model tested (fig. 1(a)) consisted of the nozzle body (fig. 1(b)), a shim (fig. 1(e) or (f)), and the 1/4-inch or 2-inch nozzle piece (fig. 1(c) or (d)) mounted together to form a configuration having a slot near the exit. A photograph of an assembled model is shown in figure 1(g). Secondary air supplied from an external source limited to 100 pounds per square inch gage and 2.2 pounds per second was injected through the slot from the annular plenum chamber in the nozzle body.

The following table summarizes the configurations tested:

Model operation	Slot width (shim thickness, X)	Slot circumference, α	Primary-pressure ratio, P_p/P_0	Secondary-pressure ratio, P_s/P_0
Variable-discharge nozzle	0.018	360	1.6 to 2.8	2.00 to 7.72
	.033	↓	↓	2.00 to 7.72
	.051			2.00 to 6.32
	.092			2.00 to 4.07
	.118			2.00 to 3.19
	.369		2.0 to 2.4	2.00 to 2.50
	.467		2.0 to 2.4	2.00 to 2.50
Jet deflector	0.103	180	1.6 to 2.8	2.00 to 3.18
	.250	90	↓	2.00 to 3.20
	.500	90		2.00 to 3.20
	.500	45		2.00 to 3.20

Experimental Setup

The experimental setup, illustrated in figure 2, can measure forces in all directions, but only the thrust and yaw components were significant in this investigation. Thrust and yaw are measured as torques about pivot points A and B, respectively, by means of diaphragm-type force cells connected to the setup through flexure members.

Instrumentation

Both the primary and secondary airflows were measured with standard ASME orifices. Total temperatures were obtained from thermocouples at the orifices. Primary inlet pressure was measured by an eight-tube total-pressure survey rake just ahead of the nozzle body. Secondary inlet pressure was measured by a calibrated gage at the nozzle body. Ambient pressure was obtained with a barometer.

The nozzle body and nozzle pieces were instrumented with 0.06-inch-diameter wall-pressure taps as required.

PROCEDURE

Calibration

The force-measuring systems were calibrated with dead weights. Leakage at the labyrinth seal surrounding pivot point B (fig. 2) was measured with air from an external source. The primary airflow was corrected for this leakage.

Performance Tests

The performance of each configuration was obtained over a primary-pressure-ratio range from 1.4 to 3.0 with secondary flows from zero to the maximum obtainable. The experimentally determined factors were computed from these data and from measured physical areas.

ANALYSIS

For convenience, all symbols and definitions used in this report are given in appendix A.

The general pattern of primary and secondary flows in this type of device is indicated in the following sketch:

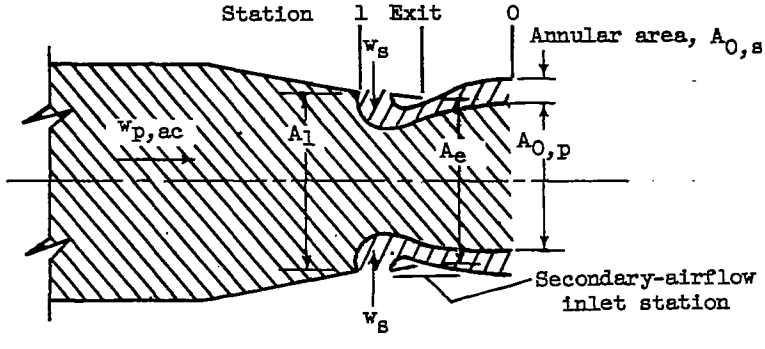

In operation, the force necessary to turn the secondary jet toward the exit is furnished by the primary gas. The reaction of this force has the same effect as an additional wall around the primary gas and serves to restrict the flow.

In the following steady-state analysis, assume that:

(1) The measured primary gas $w_{p,ac}$ expands isentropically and one-dimensionally to the upstream edge of the injection slot, station 1.

(2) Secondary gas w_s enters the nozzle with no axial momentum.

(3) Both streams together do not fill the exit station.

(4) Both streams expand isentropically and one-dimensionally to ambient pressure at station 0 (thus, the streams do not mix).

Flow Rates

The axial pressure forces acting on the flow between stations 1 and 0 are shown in the following sketch:

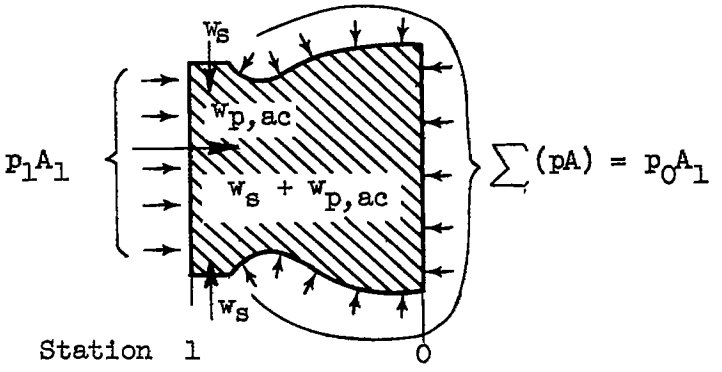

The momentum equation is

$$\frac{-w_{p,ac}}{g} V_{1,p} + \frac{w_{p,ac}}{g} V_{0,p} + \frac{w_s}{g} V_{0,s} = p_1A_1 - p_0A_1 \qquad (1)$$

Rearrangement yields an expression for the secondary weight flow w_s that permits passage of primary flow $w_{p,ac}$:

$$w_s = \frac{w_{p,ac}(V_{1,p} - V_{0,p}) + A_1g(p_1 - p_0)}{V_{0,s}} \qquad (2)$$

Because of losses (shear, mixing, etc.) in the actual system, the measured secondary weight flow $w_{s,ac}$ required to produce this effect is different by a factor f than that computed by equation (2). Thus,

$$f \equiv \frac{w_{s,ac}}{w_s} \tag{3}$$

Effective-Area Ratio

By definition, the primary-nozzle discharge coefficient C_d is

$$C_d \equiv \frac{(w_p \sqrt{\theta_p}/A_e \delta_p)_{ac}}{(w_p \sqrt{\theta_p}/A_e \delta_p)_{id,o}}$$

The same expression is written for the unrestricted-flow discharge coefficient $C_{d,o}$ and, by division,

$$\frac{C_d}{C_{d,o}} = \left(\frac{w_p}{w_{p,o}}\right)_{ac} \tag{4}$$

By definition, $A_{eff} = C_d A_e$. Therefore,

$$\frac{C_d}{C_{d,o}} = \frac{A_{eff}}{A_{eff,o}} = \left(\frac{w_p}{w_{p,o}}\right)_{ac} \tag{5}$$

By equation (2), the effective-area ratio $A_{eff}/A_{eff,o}$ is

$$\frac{A_{eff}}{A_{eff,o}} = \frac{A_1 g(p_1 - p_0) - w_s V_{0,s}}{(w_{p,o})_{ac}\,(V_{0,p} - V_{1,p})} \tag{6}$$

The relation between p_1 and $V_{1,p}$ is found by using station 1 continuity expressions.

Thrust

For the assumptions made, the secondary flow by itself produces no axial jet thrust on the system; so the isentropic jet thrust is

$$F_z = \frac{w_{p,ac}}{g} V_{1,p} + A_1(p_1 - p_0) \tag{7}$$

where $V_{1,p}$ and p_1 are isentropic terms. This relation shows that the device acts as a convergent nozzle of exit area A_1 that expands the primary gas to p_1. The expression for actual jet thrust, then, must include a coefficient to account for expansion losses up to station 1. Thus,

$$F_{z,ac} = C\left(\frac{w_{p,ac}}{g} V_{1,p} + A_1 p_1\right) - A_1 p_0 \tag{8}$$

where, by rearrangement,

$$C = \frac{F_{z,ac} + A_1 p_0}{\frac{w_{p,ac}}{g} V_{1,p} + A_1 p_1} \tag{9}$$

Because of similarity to an unchoked convergent nozzle, C is expected to be in the order of 0.98.

A measure of the efficiency of this device in producing thrust is desirable. By definition,

$$\text{Thrust ratio} = \frac{F_{z,ac}}{\frac{w_{p,ac}}{g} V_{0,p} + \frac{w_{s,ac}}{g} V_{0,s}} \tag{10}$$

Thrust ratio can be evaluated in terms of the primary-gas quantities by use of equations (8) and (2).

RESULTS AND DISCUSSION

Analytical: Variable-Area Nozzle

In this section the secondary-weight-flow ratio $w_{s,ac}/w_{p,ac}$ theoretically required to produce a given primary-nozzle effective-area ratio $A_{eff}/A_{eff,o}$ is discussed, together with the corresponding thrust ratio. (For turbojet application, $w_{s,ac}/w_{p,ac}$ would be the ratio of bleed to tailpipe flow, and $A_{eff}/A_{eff,o}$ the ratio of effective nozzle flow area with secondary flow to effective nozzle area without secondary flow.) Performance is presented for primary-pressure ratios from 2 to 8, secondary-pressure ratios from 2 to 40, a primary temperature of 1500° R, and secondary temperatures from 500° to 2500° R. Computations were made with the use of equations (2) and (10) by the method described in appendix B. The values used for nozzle discharge coefficient and specific heat ratio are given in figure 3.

In figures 4 to 6, the dashed curves show performance for $f = 1.0$, and the solid curves represent $f = 1.1$. For all curves, $C = 0.98$. These numbers are representative of the values obtained experimentally, as shown in the next section. Computations were arbitrarily stopped at $A_{eff}/A_{eff,o} = 0.5$, although values as low as 0.33 were obtained experimentally.

Effect of primary and secondary pressures. - The effect of primary and secondary pressures on the performance of a device having an injection slot at the exit is illustrated in figure 4 for primary- and secondary-gas temperatures of 1500° R. Small effective-area ratios are obtained with large secondary flow. For each primary pressure, the secondary-weight-flow ratio required to produce a given effective-area ratio is reduced as the secondary pressure is increased.

The thrust ratio is reduced along with the effective-area ratio. When $f = 1.0$, the reduction is small and the performance is acceptable at all primary and secondary pressures. However, the thrust ratio decreases when $f = 1.1$.

Effect of temperature. - The effect of secondary-gas temperature on the performance of this device is illustrated in figure 5. Raising the temperature increases $V_{0,s}$ and reduces the secondary-weight-flow ratio required to produce a given effective-area ratio. Because this effect is more significant when the effective-area ratio is small, it may be desirable to burn in the secondary for such operation.

The thrust ratio is independent of secondary-gas temperature and is the same as in figure 4(b).

Effect of injection-slot location. - The effect of the secondary-gas injection-slot location on the performance is illustrated in figure 6 for 1500° R primary- and secondary-gas temperatures. Moving the injection-slot location upstream from the exit increases the secondary-weight-flow ratio required to produce a given effective-area ratio. Thus, for most efficient use of the secondary gas, the injection station must be at the nozzle exit.

The thrust ratio is again the same as in figure 4(b).

Experimental: Variable-Area Nozzle

The pressures within and at the exit of one of the configurations tested are shown in figure 7. Measured wall pressures agree reasonably well with those computed from one-dimensional isentropic flow relations except at station 1. However, at this station the quantity $\frac{w_{p,ac}}{g} V_{1,p} + p_1 A_1$ is very nearly the same when computed with either

the measured or isentropic wall pressure; thus assumption (1) of the preceding analysis is valid. Figure 7 also shows that the pressure in the vicinity of the exit is sufficiently close to permit assumption of ambient wall pressure downstream of the injection slot.

Basic performance. - The performance of all the configurations tested is given in table I, and the performance of a typical configuration (slot width X, 0.051 in.) is plotted in figure 8. The effective-area ratio is based on the effective area of the nozzle exit, and thus the values given are somewhat greater than if the injection slot had been placed at the exit. As shown in figure 8, for constant primary-pressure ratio, the effective-area ratio and the thrust ratio decrease and the secondary-weight-flow ratio increases as secondary pressure is raised. The dashed and dot-dashed curves in the figure show the performance that would be obtained at $P_s/p_0 = 6.32$ and 2.5, respectively, for $f = 1.0$. The difference between these curves and the corresponding data curves shows the extent to which factor f reduces the performance (for these configurations, f varied between 1.03 and 1.22, as indicated in table I).

Although not shown in figure 8, the performance of the device was the same when the 2-inch nozzle piece (fig. 1(d)) was mounted, except that the thrust ratio was further reduced because of shocks in the nozzle piece. These shocks might not have occurred if the flow passage had been divergent; however, no tests were made with a convergent-divergent version of this device.

The effective-area ratio can be continuously varied by changing either the secondary pressure or the slot width, as shown in figure 9. At constant secondary pressure, the effective-area ratio decreases almost linearly as the slot width is increased (fig. 9(a)). For constant slot width, the effective-area ratio is smoothly, but not linearly, reduced as the secondary pressure is increased (fig. 9(b)).

Evaluation of factor f. - The factor f, evaluated for each test point by means of equations (2) and (3), was empirically correlated with the station 1 velocity ratio, as shown in figure 10. Station 1 velocity ratio $V_{1,s}/V_{1,p}$ is the ratio of the secondary- (limited to sonic) and primary-jet velocities that could be obtained with isentropic primary static pressure at the upstream edge of the injection slot. The factor f is nearly unity when this ratio is about 2; when the ratio is 5, indicating high secondary pressure and small effective-area ratio, f is about 1.15. It should be emphasized that these values were obtained with unheated flows, zero axial secondary inlet momentum, and a continuous injection slot. The effects on f of changes in these conditions were not determined.

Evaluation of coefficient C. - The coefficient C, evaluated for each test point by means of equation (9), is shown as a function of the station 1 velocity ratio in figure 11. With only a few exceptions, the value 0.98 correlates all data obtained within 1 percentage point.

Evaluation of slot discharge coefficient $C_{d,slot}$. - The variation of injection-slot discharge coefficient $C_{d,slot}$ with effective-secondary-pressure ratio is shown in figure 12. Effective-secondary-pressure ratio is the secondary total pressure P_s divided by the average slot exhaust pressure, $\frac{1}{2}(p_1 + p_0)$. A single curve generalizes all data obtained with with accuracy sufficient for design purposes.

4829

Experimental: Jet Deflector

A jet deflector can be used to provide reaction control to augment or supplant the forces produced by conventional control surfaces. The aerodynamic nozzle was operated as a deflector by injecting the secondary air in only one side of the nozzle with the shims shown in figure 1(f). The pressures within one of the configurations tested in this manner are shown in figure 13. On the side containing the slot, the wall pressure is high because the primary flow is restricted. On the other side, the wall pressure is more nearly that which would be obtained with unrestricted primary flow. Thus, a measurable side force is produced by the pressure difference between the opposite nozzle walls plus the secondary-jet momentum. The ratio of measured side force F_S to total isentropic jet thrust $\frac{w_{p,ac}}{g} V_{0,p} + \frac{w_{s,ac}}{g} V_{0,s}$ is called side-force ratio, while thrust ratio has the same meaning as given previously.

CJ-2

The performance of configurations operated as jet deflectors is given in table II, and the performance of a typical configuration is plotted in figure 14. The dashed curves in this figure represent the side-force ratio that could be obtained by exhausting the secondary airflow used by the 90° α, 3.2 P_s/p_0 configuration through a convergent nozzle into still air. At lower values of secondary airflow, the side-force ratio produced by this device is greater than the dashed curves because of the wall-pressure forces. As the secondary airflow is increased, this effect is counteracted by reduced secondary-jet momentum caused by the increased static pressure at station 1. Figure 14 shows also that the effective-area ratio is substantially reduced for significant values of side force; consequently, the use of this type of deflector probably would be limited in use to producing trim forces.

CONCLUDING REMARKS

A simplified theoretical analysis showed that considerably reduced effective flow area can be obtained in a convergent exhaust nozzle by

injecting a high-pressure, high-temperature secondary jet into the nozzle at the exit. The secondary-flow rate theoretically required to produce a given effect must be increased by a factor f, in the actual case, because of losses. The thrust ratio (ratio of actual thrust to the thrust attainable from primary and secondary isentropic expansion) depends on f and is reduced 2 percent because of normal nozzle losses.

The performance of a device of this type was experimentally investigated with a 4-inch-exit-diameter nozzle having a continuous circumferential injection slot, unheated pressurized air discharged to atmosphere, and primary- and secondary-pressure ratios from 1.6 to 2.8 and from 2.0 to 7.7, respectively. The effective flow area was reduced as much as 67 percent, while the thrust ratio was 0.94 or better in nearly all cases. Design coefficients were correlated with easily measured or computed parameters.

Significant values of side force were obtained by injecting the secondary jet on only one side of the nozzle. In most cases, the performance of this device is better than could be obtained by exhausting the same gas into still air. The reduction of effective flow area, however, is so large as to probably limit application.

Lewis Flight Propulsion Laboratory
National Advisory Committee for Aeronautics
Cleveland, Ohio, April 18, 1958

APPENDIX A

SYMBOLS AND DEFINITIONS

Symbols

A	area, sq ft
C	experimentally determined coefficient (see eq. (9))
C_d	discharge coefficient
F	force or jet thrust, lb
f	experimentally determined factor (see eq. (3))
g	acceleration due to gravity, ft/sec^2
M	Mach number
P	total pressure, lb/sq ft
p	static pressure, lb/sq ft
R	gas constant, $ft/^oR$
T	total temperature, ^oR
V	velocity, ft/sec
w	weight-flow rate, lb/sec
X	shim thickness, in.
α	slot circumference, deg
γ	ratio of specific heats at total temperature of fluid
δ	ratio of total pressure to NACA standard sea-level pressure of 2116 lb/sq ft
θ	ratio of total temperature to NACA standard sea-level temperature of 518.7^o R

Subscripts:

ac	actual

4829

CJ-2 back

e	exit
eff	effective
id	ideal
o	at unrestricted flow conditions
p	primary
S	side (perpendicular to axial direction)
s	secondary
slot	slot
w	wall
z	in axial direction
0	ambient, or station at which flow has expanded to ambient pressure
1	station at upstream edge of injection slot

Definitions

A_{eff}	$C_d A_e$
$A_{eff}/A_{eff,o}$	effective-area ratio, same as $C_d/C_{d,o}$
C_d	at same pressure ratio, the ratio of actual corrected flow per unit of actual exit area to one-dimensional isentropic flow per unit of actual exit area (minimum area at exit)
F_S	moment about pivot point B divided by distance between pivot point B and nozzle exit
F_z	isentropic axial jet thrust
$F_{z,ac}$	actual axial jet thrust
$\dfrac{F_{z,ac}}{\frac{w_{p,ac}}{g} V_{0,p} + \frac{w_{s,ac}}{g} V_{0,s}}$	thrust ratio

P_p/p_0	primary-pressure ratio
P_s/p_0	secondary-pressure ratio
w_p	primary-weight-flow rate, computed from one-dimensional isentropic flow relations
$w_{p,ac}$	actual (measured) primary-weight-flow rate
w_s	secondary-weight-flow rate, computed from one-dimensional isentropic flow relations
$w_{s,ac}$	actual (measured) secondary-weight-flow rate
$w_{s,ac}/w_{p,ac}$	secondary-weight-flow ratio
$(w\sqrt{\theta}/A_e\delta)_{ac}$	corrected flow per unit of actual exit area

APPENDIX B

METHOD OF SOLVING EQUATION (2)

First choose P_p/p_0, T_p, γ_p, R_p, and $C_{d,o}$. Solve by any convenient method for the unrestricted weight flow $w_{p,o}$ in terms of p_0 and A_e. In addition, choose A_1/A_e and $w_p/w_{p,o}$. Solve for M_1, using

$$\frac{w_p\sqrt{T_p}}{A_1 P_p} = \sqrt{\frac{\gamma_p g}{R_p}}\left[\frac{M_1}{\left(1 + \frac{\gamma_p - 1}{2} M_1^2\right)^{(\gamma_p+1)/2(\gamma_p-1)}}\right] \tag{B1}$$

from which

$$p_1 = P_p\left(1 + \frac{\gamma_p - 1}{2} M_1^2\right)^{-\gamma_p/\gamma_p-1} \tag{B2}$$

Choose P_s/p_0, T_s, γ_s, and R_s. Find $V_{1,p}$, $V_{0,p}$, and $V_{0,s}$ by using p_1/P_p, p_0/P_p, and p_0/P_s, respectively. Reference 3 is helpful in making these computations. Finally, substitute all terms in equation (2) and solve for w_s.

REFERENCES

1. Hawthorne, Randolph: Jet Exhaust Controlled by "Striction" Nozzle. Aviation Age, vol. 27, no. 1, Jan. 1957, pp. 46-49.

2. Martin, A. I.: The Aerodynamic Variable Nozzle. Jour. Aero. Sci., vol. 24, no. 5, May 1957, pp. 357-362.

3. Turner, L. Richard, Addie, Albert N., and Zimmerman, Richard H.: Charts for the Analysis of One-Dimensional Steady Compressible Flow. NACA TN 1419, 1948.

TABLE I. - PERFORMANCE OF VARIABLE-DISCHARGE EXHAUST NOZZLE[a]

[This table contains all configurations for which values of f, C, and $C_{d,slot}$ are reported herein.]

Slot width, in.	Secondary-pressure ratio, P_s/P_0	Primary-pressure ratio, P_p/P_0	Secondary-weight-flow ratio, $w_{s,ac}/w_{p,ac}$	Effective-area ratio, $A_{eff}/A_{eff,o}$ (b)	Thrust ratio	Experimental factor, f	Experimental coefficient, C	Slot discharge coefficient, $C_{d,slot}$
0.018	7.72	1.6	0.150	0.601	0.935	1.054	0.978	0.977
		2.0	.093	.743	.961	.987	.978	.973
		2.4	.069	.826	.963	.988	.976	.970
		2.8	.057	.865	.972	.940	.977	.961
	6.32	1.6	.108	.666	.949	1.038	.981	.950
		2.0	.070	.792	.959	.970	.976	.948
		2.4	.053	.866	.959	.995	.973	.944
		2.8	.043	.898	.967	.945	.975	.937
	4.24	1.6	.062	.770	.945	1.042	.978	.939
		2.0	.042	.873	.951	.998	.972	.936
		2.4	.031	.932	.954	1.097	.972	.933
		2.8	.027	.955	.968	1.080	.975	.920
	2.50	2.0	.021	.965	.967	1.246	.983	.815
		2.4	.014	.991	.959	1.177	.975	.755
	2.00	2.0	.014	.965	.961	1.146	.978	.746
0.033	7.72	1.6	0.373	0.436	0.894	1.144	0.977	0.960
		2.0	.204	.615	.949	1.069	.980	.960
		2.4	.146	.716	.956	1.039	.977	.960
		2.8	.116	.773	.968	.990	.977	.943
	6.32	1.6	.258	.515	.908	1.125	.974	.958
		2.0	.152	.674	.951	1.043	.976	.957
		2.4	.110	.769	.956	1.029	.975	.956
		2.8	.088	.821	.963	.996	.974	.950
	4.22	1.6	.138	.638	.948	1.030	.980	.948
		2.0	.087	.778	.959	.997	.977	.948
		2.4	.065	.858	.959	1.029	.975	.945
		2.8	.054	.888	.974	.952	.980	.936
	3.16	1.6	.084	.738	.954	1.037	.982	.895
		2.0	.056	.853	.960	1.026	.978	.893
		2.4	.043	.923	.956	1.146	.975	.886
		2.8	.035	.949	.967	1.164	.980	.862
	2.50	2.0	.040	.916	.966	1.226	.985	.875
		2.4	.029	.966	.965	1.239	.980	.792
	2.00	2.0	.025	.972	.960	1.457	.980	.728
0.051	6.32	1.6	0.638	0.329	0.912	1.097	0.983	0.976
		2.0	.300	.539	.948	1.050	.980	.978
		2.4	.203	.660	.956	1.038	.977	.973
		2.8	.154	.736	.961	1.031	.977	.965
	4.24	1.6	.270	.514	.941	1.068	.984	.966
		2.0	.156	.686	.947	1.088	.975	.965
		2.4	.113	.783	.956	1.060	.975	.959
		2.8	.089	.838	.967	1.043	.980	.945
	3.18	1.6	.165	.622	.951	1.043	.982	.952
		2.0	.102	.773	.954	1.048	.974	.950
		2.4	.073	.859	.963	1.067	.980	.932
		2.8	.054	.905	.977	1.078	.986	.763
	2.50	2.0	.068	.842	.967	1.047	.982	.875
		2.4	.044	.932	.964	1.219	.982	.831
	2.00	2.0	.039	.942	.958	1.481	.982	.710
0.092	4.07	2.0	0.356	0.520	0.957	1.024	0.981	0.963
		2.4	.235	.650	.956	1.023	.978	.958
		2.8	.167	.740	.970	1.019	.982	.903
	3.17	2.0	.215	.647	.954	1.058	.981	.925
		2.4	.147	.764	.958	1.093	.981	.900
		2.8	.094	.846	.970	1.074	.986	.747
	2.50	1.6	.242	.572	.950	1.048	.984	.902
		2.0	.131	.758	.954	1.087	.980	.839
		2.4	.080	.878	.960	1.233	.983	.721
	2.00	1.6	.144	.695	.965	1.066	.989	.824
		2.0	.088	.875	.982	1.203	.985	.652
0.118	3.19	1.6	0.615	0.368	0.924	1.105	0.987	0.918
		2.0	.299	.572	.957	1.029	.981	.896
		2.4	.187	.712	.955	1.054	.978	.842
		2.8	.125	.807	.967	1.079	.984	.745
	2.50	1.6	.336	.507	.935	1.077	.982	.881
		2.0	.165	.716	.954	1.085	.982	.796
		2.4	.096	.847	.956	1.171	.980	.660
	2.00	2.0	.087	.850	.954	1.236	.982	.644
0.369	2.50	2.4	0.255	0.699	0.949	1.194	0.988	0.462
	2.00	2.0	.215	.714	.956	1.231	.994	.431
0.467	2.50	2.4	0.313	0.666	0.948	1.230	0.996	0.429
	2.50	2.4	.317	.655	.960	1.174	.998	.426
	2.02	2.0	.282	.678	.942	1.301	.996	.418
	2.00	2.0	.229	.713	.945	1.286	.992	.361

[a]With 1/4-inch nozzle piece mounted downstream of slot.

[b]$A_{eff}/A_{eff,o}$ based on A_e. Injection station at 1.03 A_e.

TABLE II. - PERFORMANCE OF NOZZLE[a] OPERATED AS A JET DEFLECTOR

Slot width, in.	Slot circumference, α, deg	Secondary-pressure ratio, P_s/p_0	Primary-pressure ratio, P_p/p_0	Ratio of secondary to unrestricted primary weight flow, $\frac{w_{s,ac}}{(w_{p,o})_{ac}}$	Side-force ratio	Thrust ratio	Effective-area ratio, $A_{eff}/A_{eff,o}$ (b)	Secondary-weight-flow ratio, $w_{s,ac}/w_{p,ac}$
0.103	180	3.18	1.6	0.104	0.175	0.930	0.650	0.160
			2.0	.079	.109	.947	.782	.101
			2.4	.061	.064	.961	.857	.070
			2.8	.047	.031	.972	.900	.053
		2.50	1.6	.079	.135	.942	.738	.109
			2.0	.056	.075	.948	.856	.066
			2.4	.038	.026	.952	.923	.042
		2.00	1.6	.058	.095	.941	.820	.069
			2.0	.035	.034	.953	.930	.038
0.250	90	3.20	1.6	0.120	0.231	0.888	0.656	0.185
			2.0	.088	.152	.926	.785	.113
			2.4	.066	.102	.947	.854	.076
			2.8	.048	.064	.956	.901	.054
		2.50	1.6	.086	.181	.920	.738	.118
			2.0	.058	.108	.950	.853	.067
			2.4	.037	.058	.962	.921	.040
		2.00	1.6	.059	.131	.934	.824	.072
			2.0	.032	.065	.953	.929	.029
0.500	90	3.20	1.6	0.219	0.297	0.809	0.555	0.389
			2.0	.156	.199	.896	.705	.224
			2.4	.115	.134	.930	.790	.147
			2.8	.085	.088	.949	.854	.100
		2.50	1.6	.157	.236	.914	.654	.237
			2.0	.104	.139	.930	.792	.132
			2.4	.067	.078	.947	.880	.075
		2.00	1.6	.105	.168	.920	.753	.146
			2.0	.060	.081	.920	.881	.099
0.500	45	3.20	1.6	0.110	0.179	0.876	0.733	0.152
			2.0	.080	.125	.926	.828	.098
			2.4	.060	.084	.996	.884	.066
			2.8	.044	.056	.953	.919	.047
		2.50	1.6	.079	.143	.905	.800	.099
			2.0	.052	.088	.942	.889	.059
			2.4	.035	.052	.955	.932	.038
		2.00	1.6	.053	.110	.934	.852	.063
			2.0	.030	.056	.950	.938	.032

[a]With 1/4-inch nozzle piece mounted downstream of injection slot.

[b]$A_{eff}/A_{eff,o}$ based on A_e. Injection station at 1.03 A_e.

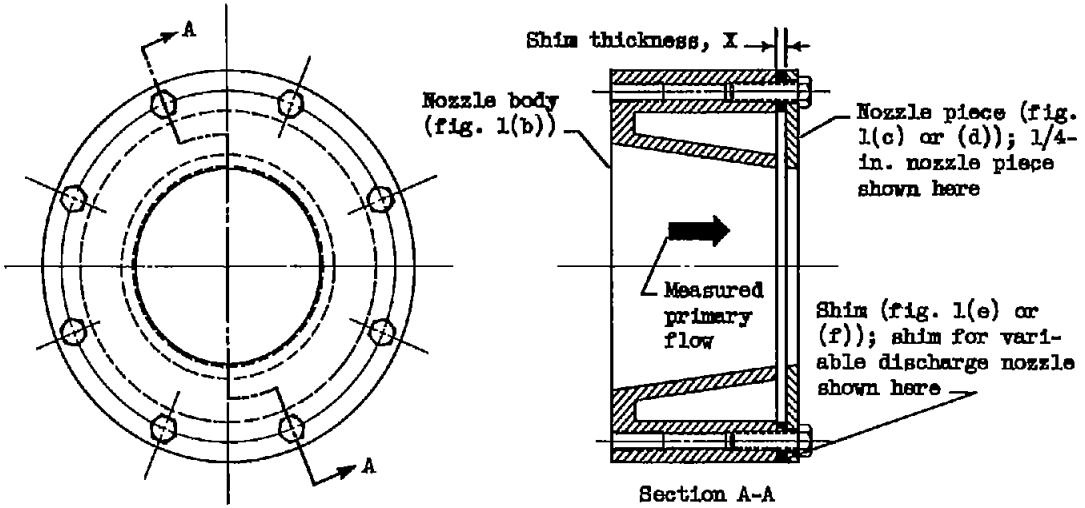

(a) Assembly.

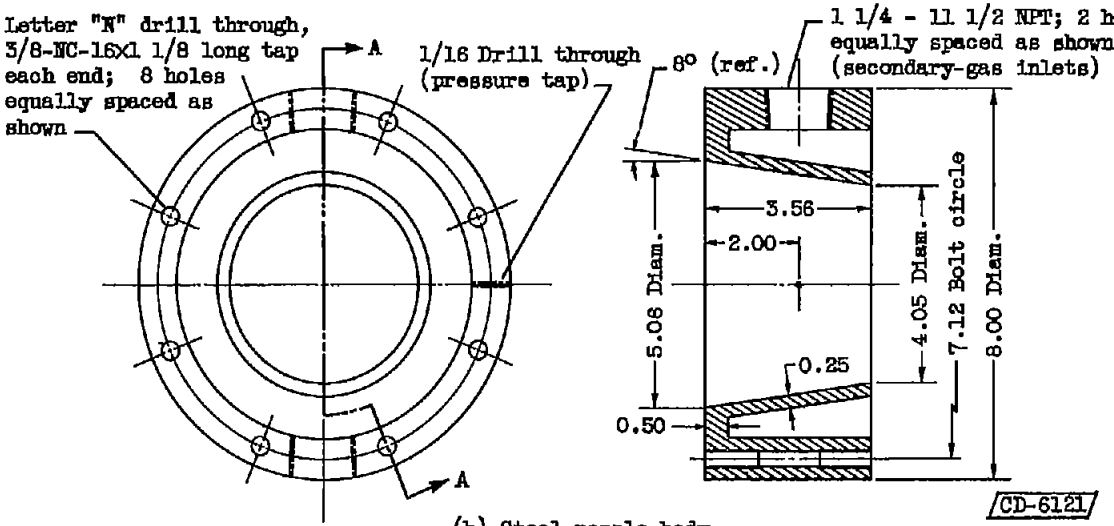

(b) Steel nozzle body.

Figure 1. - Model used in experimental part of investigation. (All dimensions in inches.)

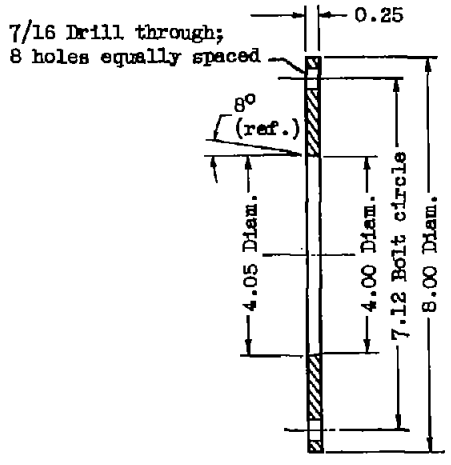

(c) Steel 1/4-inch nozzle piece.

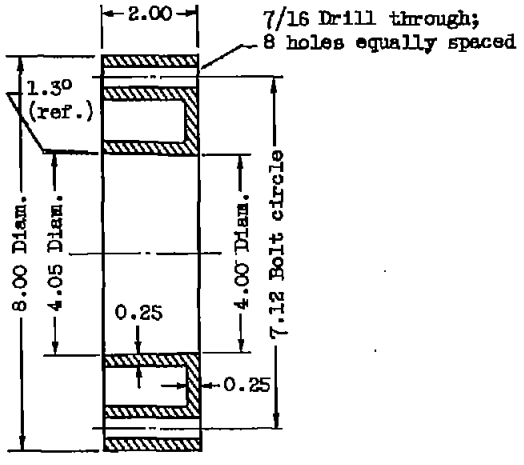

(d) Steel 2-inch nozzle piece.

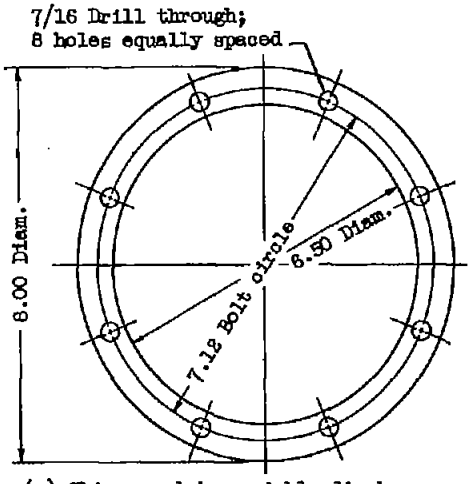

(e) Shims used in variable-discharge-nozzle investigation. Compressible material; thickness measured after assembly.

Part	Shim thickness, X, in.
1	0.018
2	.033
3	.051
4	.092
5	.118
6	.369
7	.467

Part	Shim thickness, X, in.	Slot circumference, α, deg
8	0.103	180
9	.250	90
10	.500	90
11	.500	45

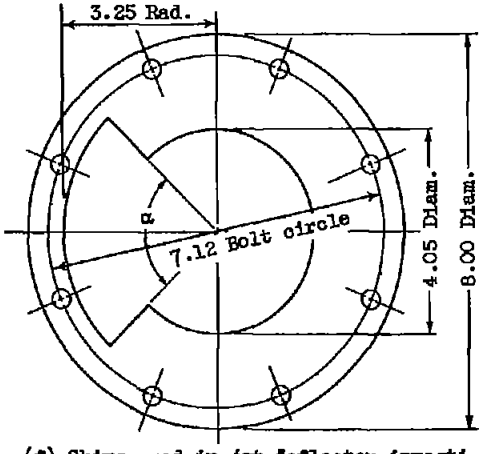

(f) Shims used in jet-deflector investigation. Compressible material; thickness measured after assembly.

CD-6122

Figure 1. - Continued. Model used in experimental part of investigation. (All dimensions in inches.)

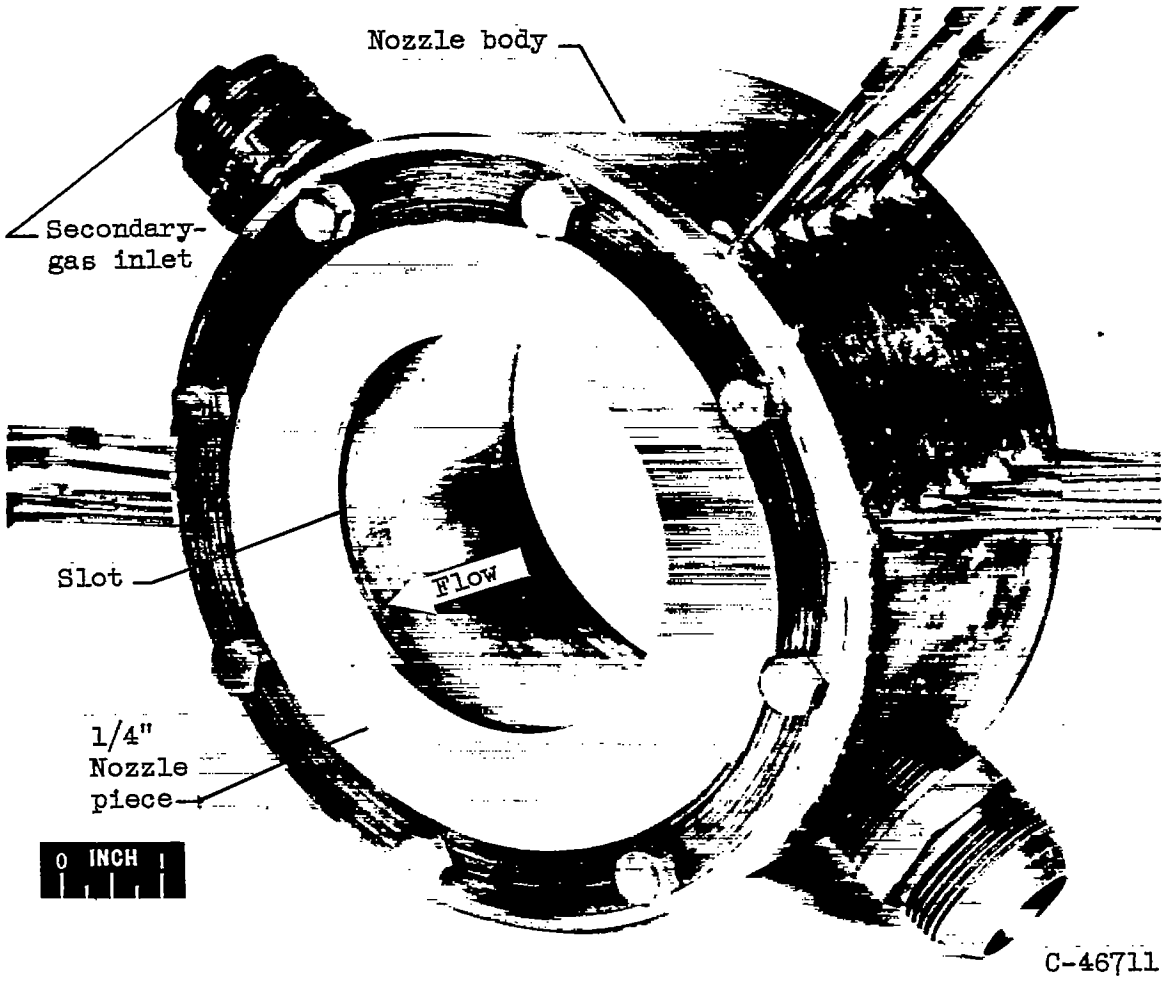

(g) Assembled model.

Figure 1. - Concluded. Model used in experimental part of investigation. (All dimensions in inches.)

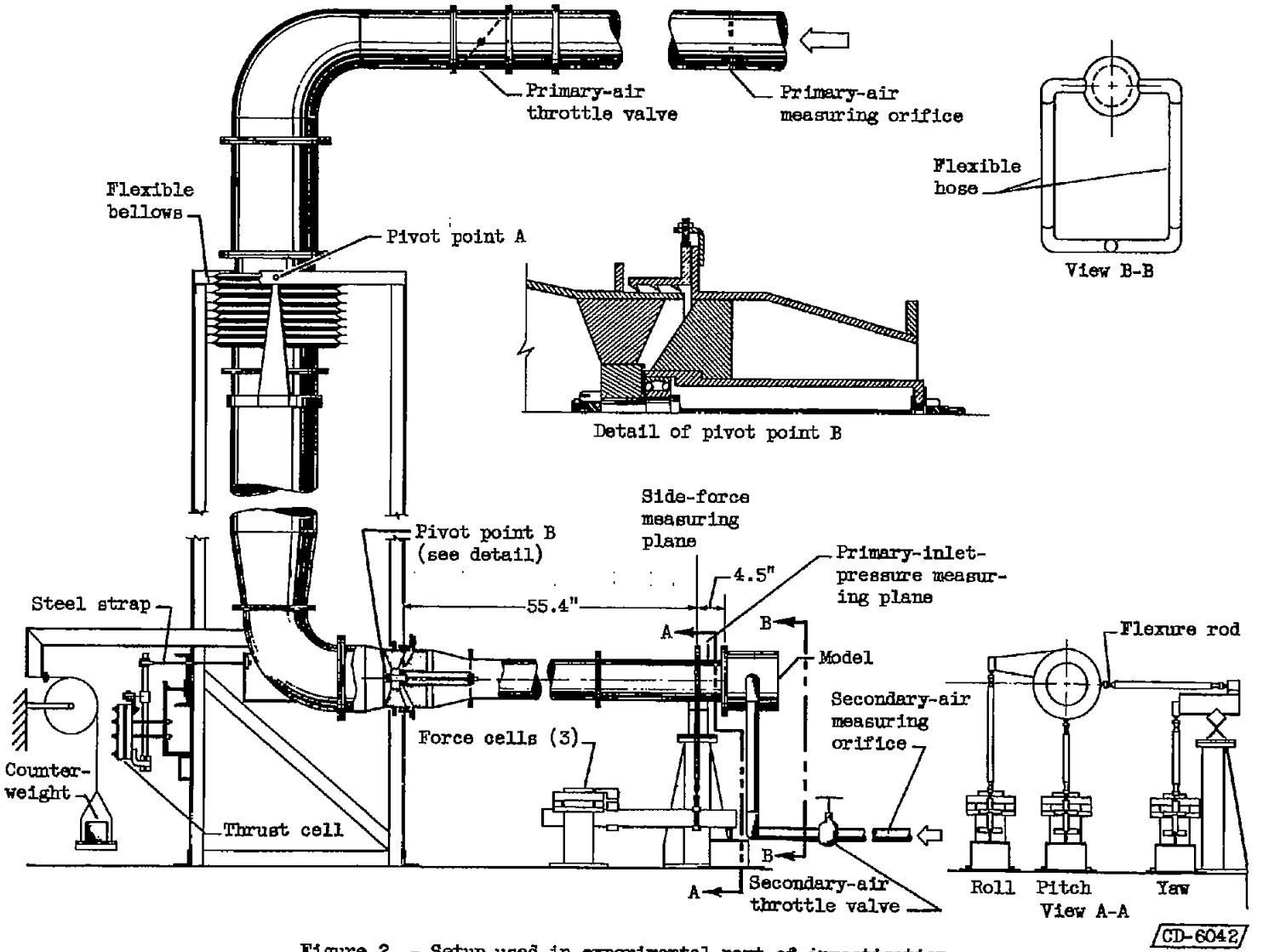

Figure 2. - Setup used in experimental part of investigation.

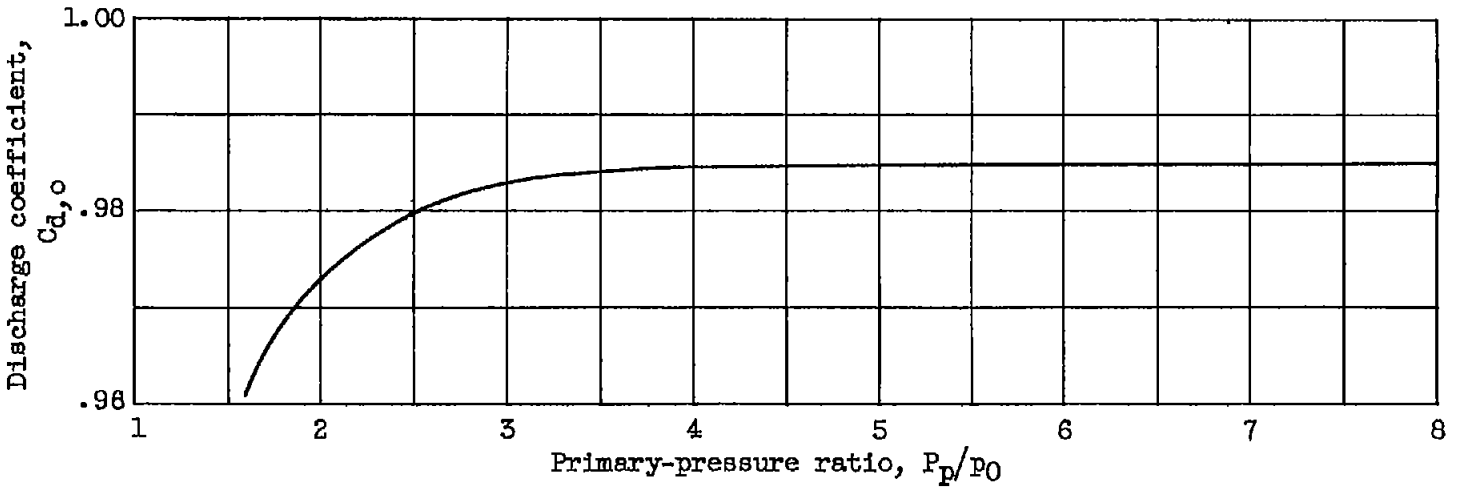

(a) Nozzle discharge coefficient. 8° Conical convergent nozzle.

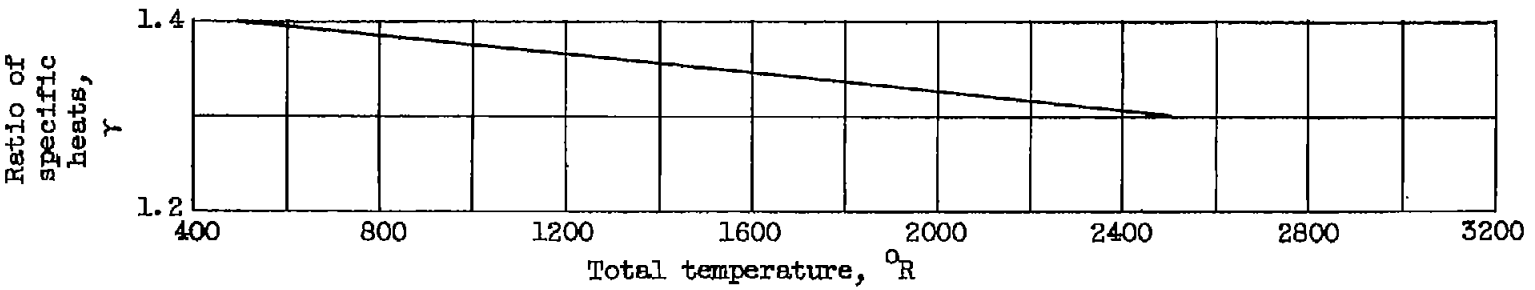

(b) Ratio of specific heats.

Figure 3. - Relations between dependent variables used in analytical computations.

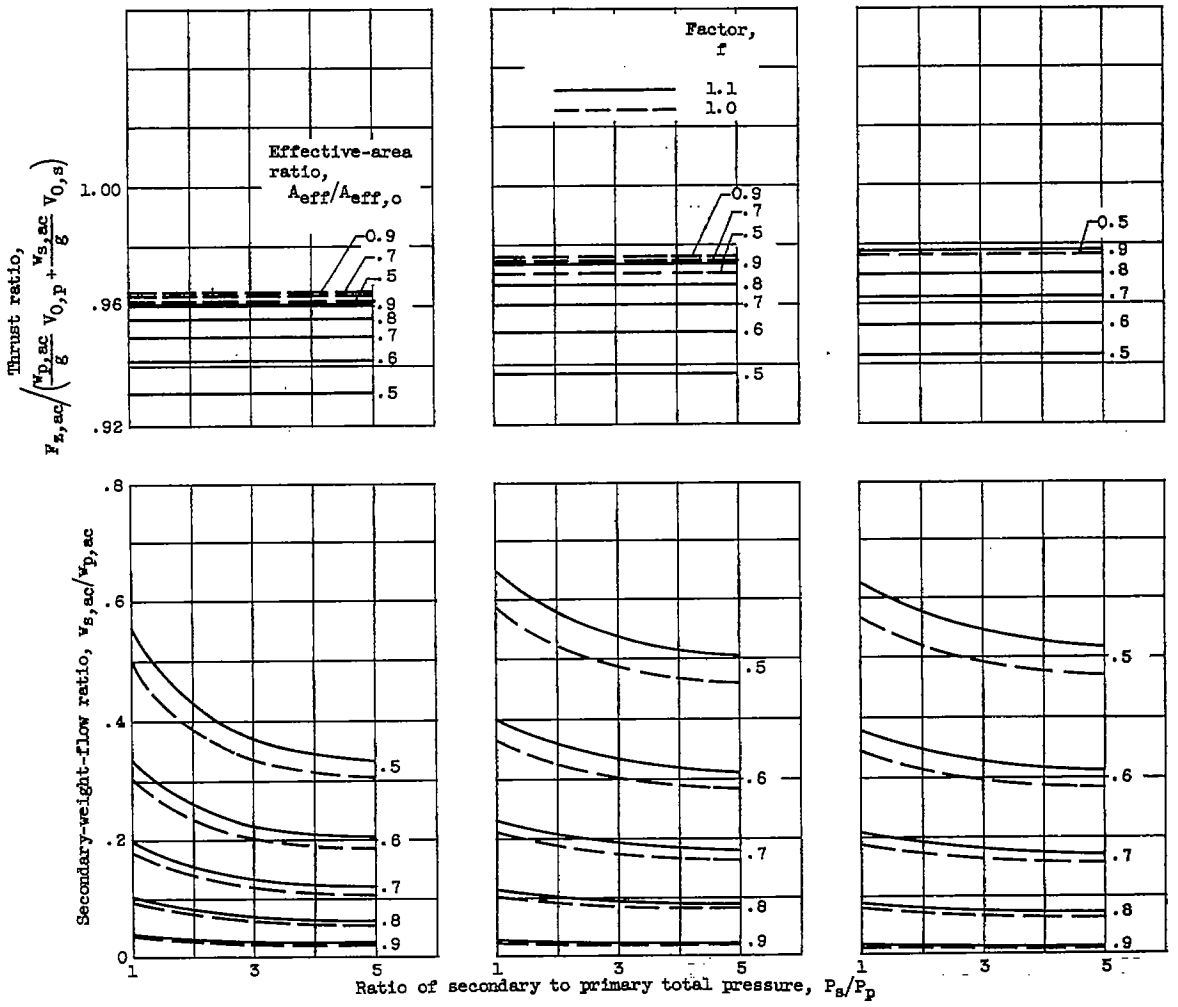

(a) Primary-pressure ratio, 2.0.

(b) Primary-pressure ratio, 5.0.

(c) Primary-pressure ratio, 8.0.

Figure 4. - Effect of primary and secondary pressures on performance. $T_s = T_p = 1500^\circ$ R; $\gamma_s = \gamma_p = 1.35$; $R_s = R_p = 53.3$ feet per $^\circ$R; $A_1 = A_e$; $C = 0.98$.

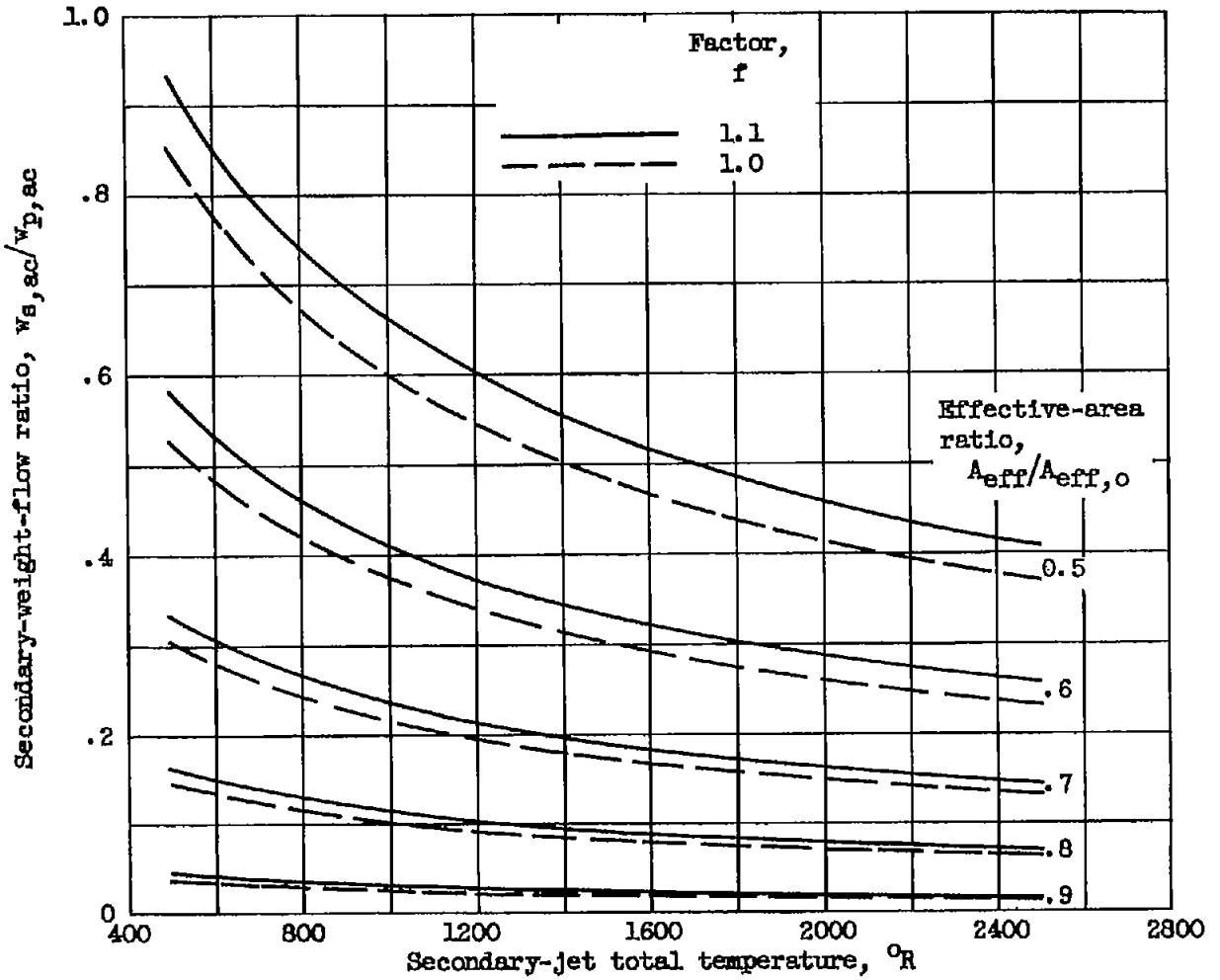

Figure 5. - Effect of secondary-jet total temperature on performance. $P_p/p_0 = 5.0$; $P_s/P_p = 3.0$; $T_p = 1500^\circ$ R; $\gamma_p = 1.35$; $R_s = R_p = 53.3$ feet per °R; $A_1 = A_e$; $C = 0.98$.

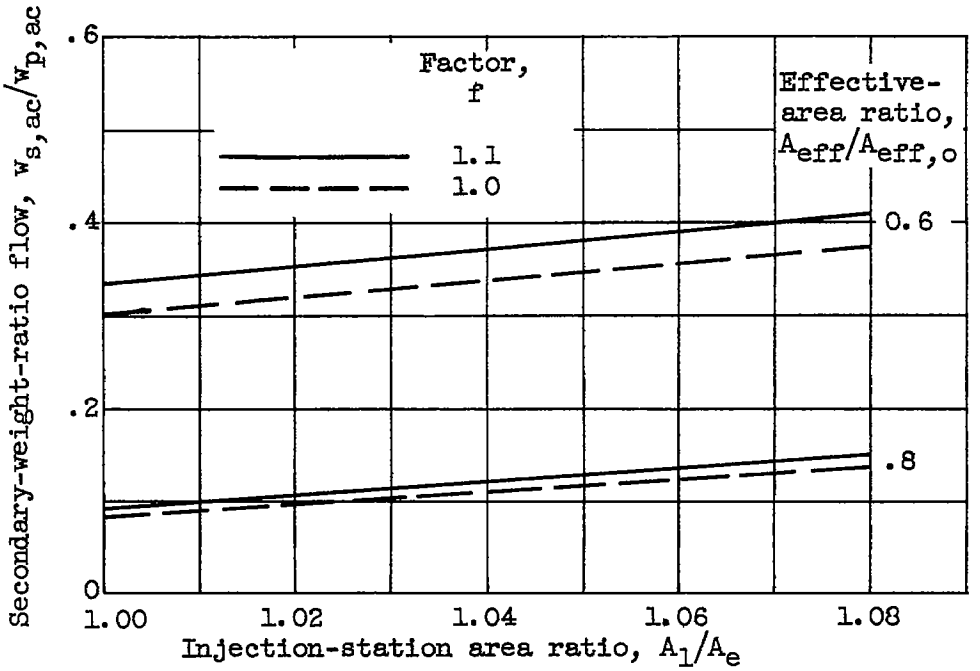

Figure 6. - Effect of injection-slot location on performance. $P_p/p_0 = 5.0$; $P_s/P_p = 3.0$; $T_s = T_p = 1500^\circ$ R; $\gamma_s = \gamma_p = 1.35$; $R_s = R_p = 53.3$ feet per $^\circ$R; C = 0.98.

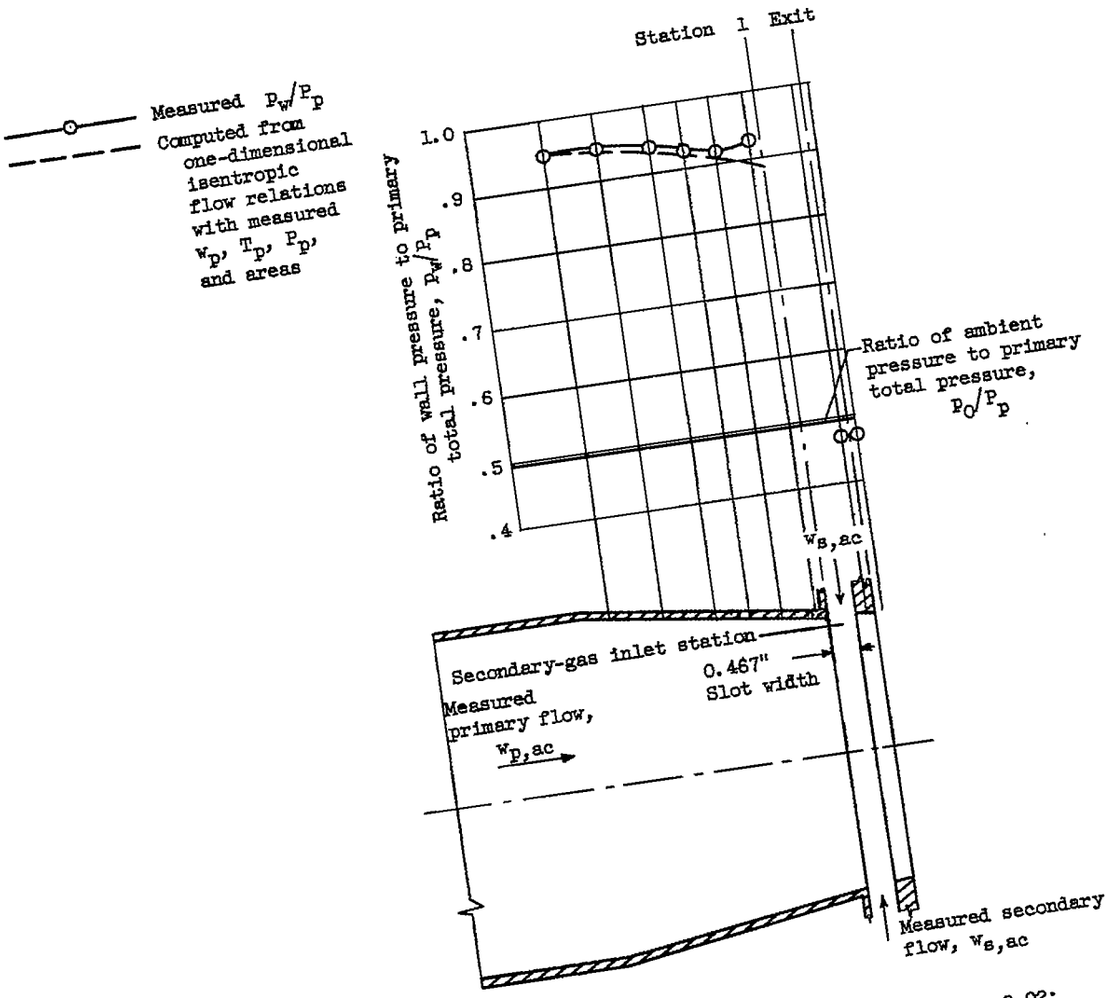

Figure 7. - Nozzle-wall-pressure distribution. $P_p/P_o = 2.02$; $P_s/P_o = 2.02$; $w_{s,ac}/w_{p,ac} = 0.268$; $A_{eff}/A_{eff,o} = 0.684$.

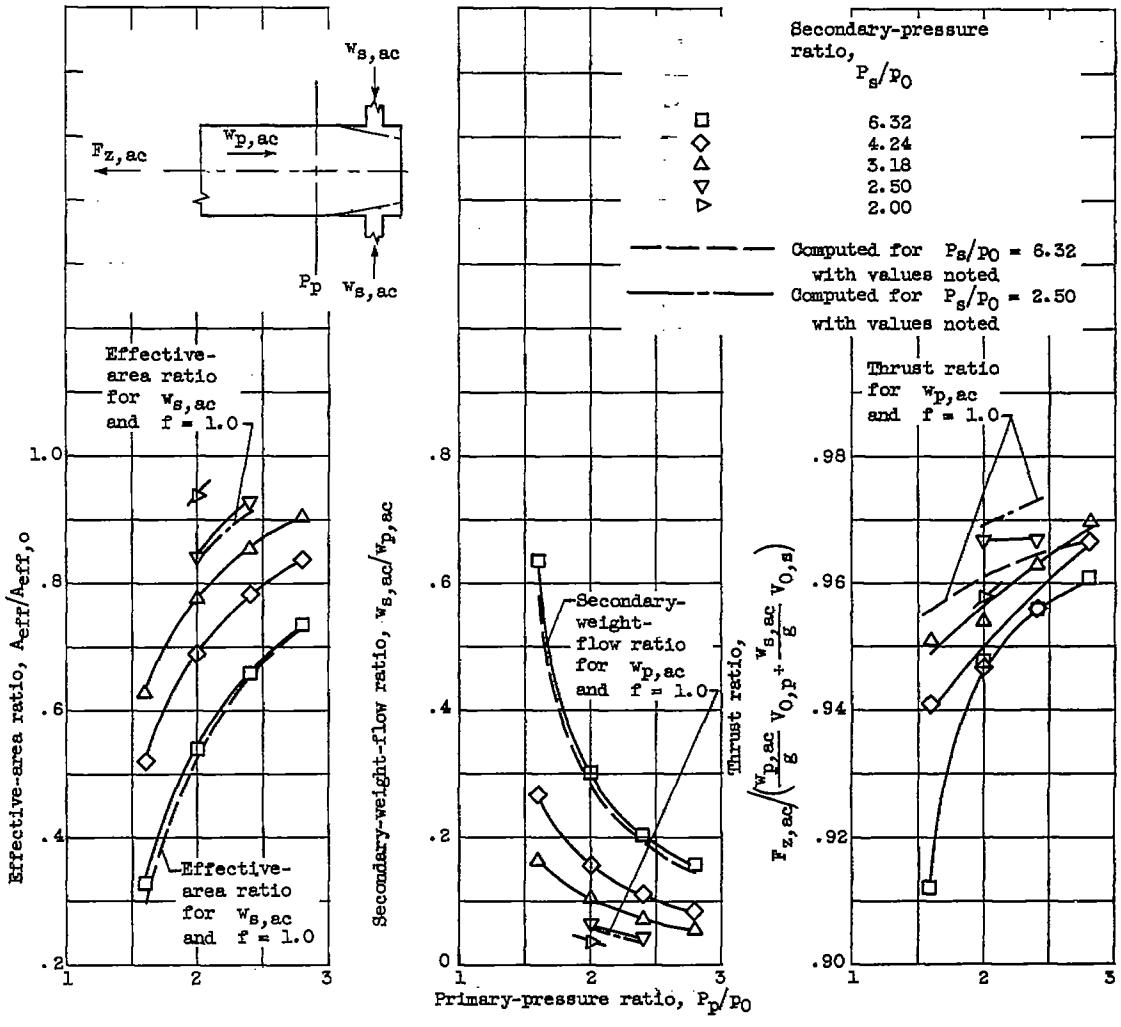

(a) Effective-area ratio. (b) Secondary-weight-flow ratio. (c) Thrust ratio.

Figure 8. - Performance of typical nozzle. $T_s \cong T_p \cong 530^\circ$ R; slot width, 0.051 in.; length downstream of slot, 0.25 in.; A_1/A_e = 1.03.

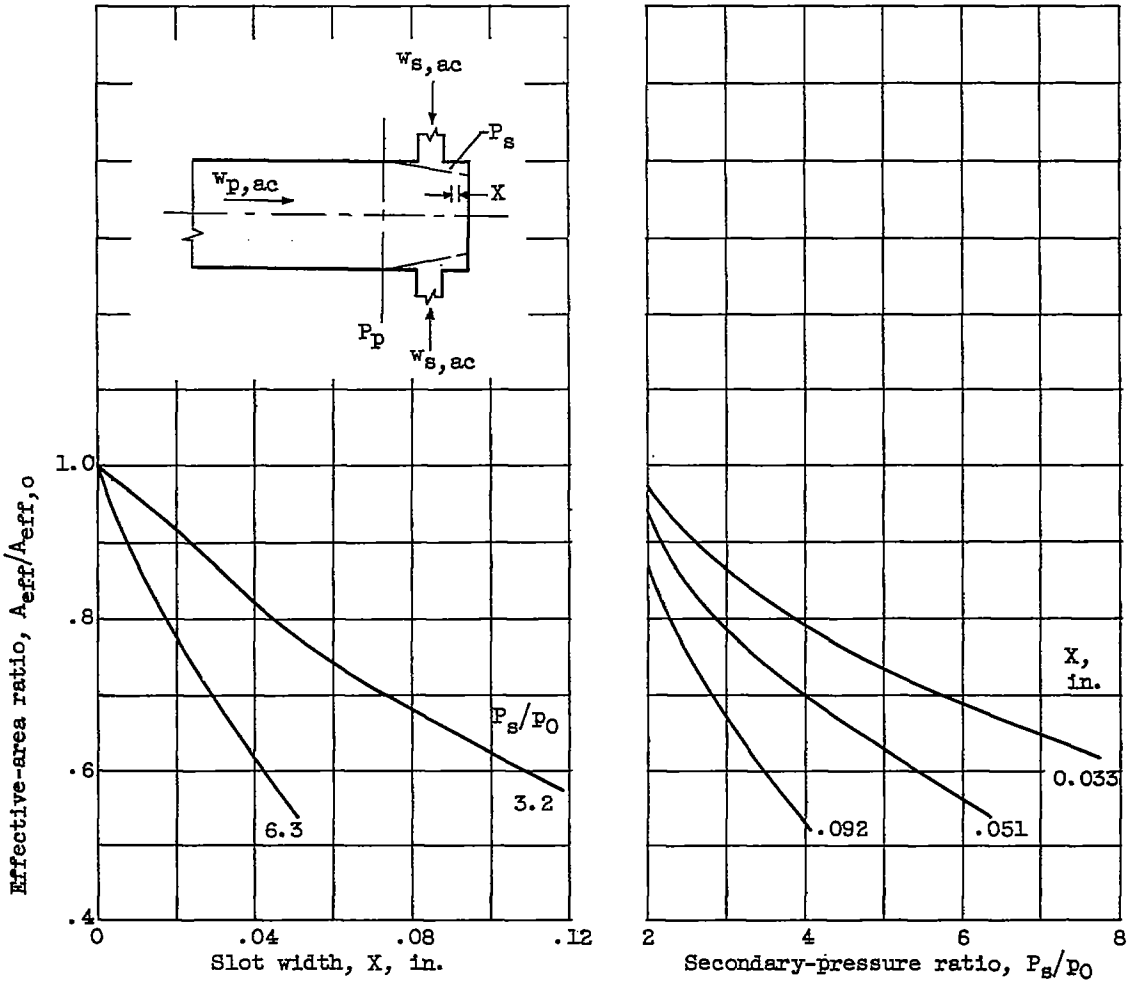

(a) Slot width. (b) Secondary-pressure ratio.

Figure 9. - Methods of varying effective-area ratio. Primary-pressure ratio, 2.0. Data taken from table I.

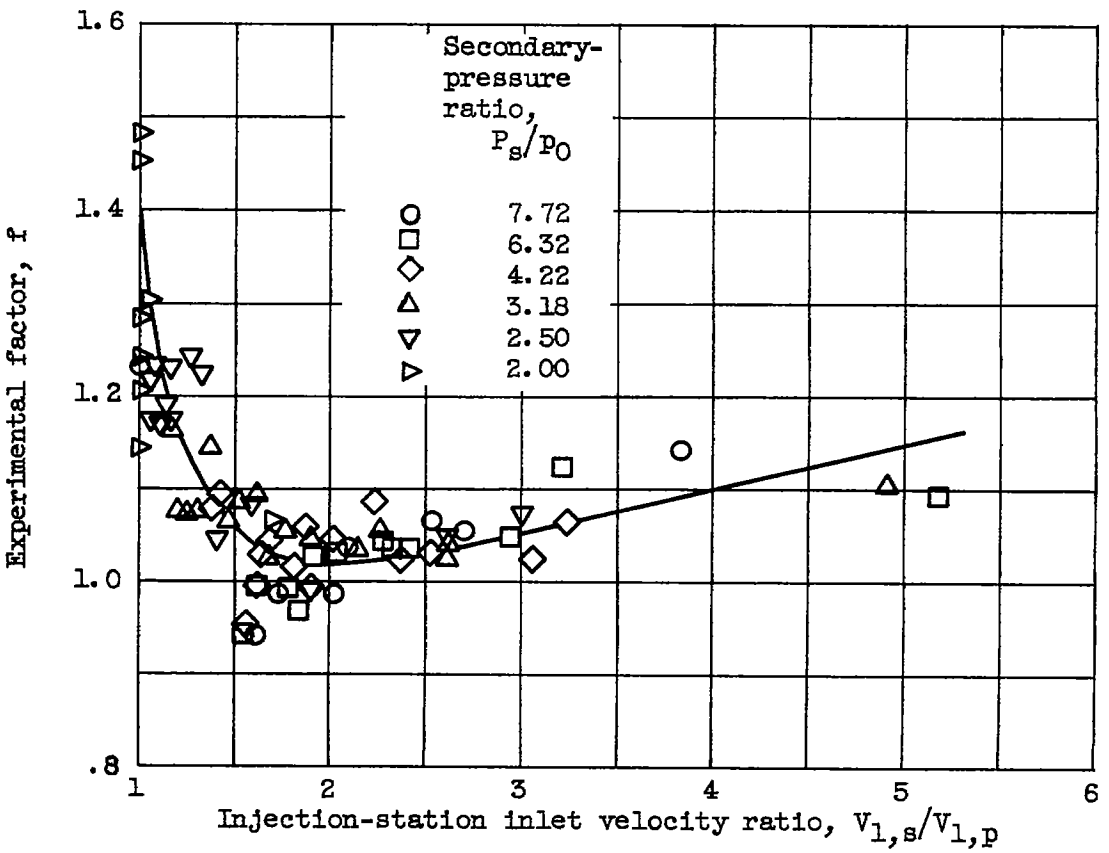

Figure 10. - Evaluation of experimental factor f for all slot widths. $T_s \cong T_p \cong 530^\circ$ R.

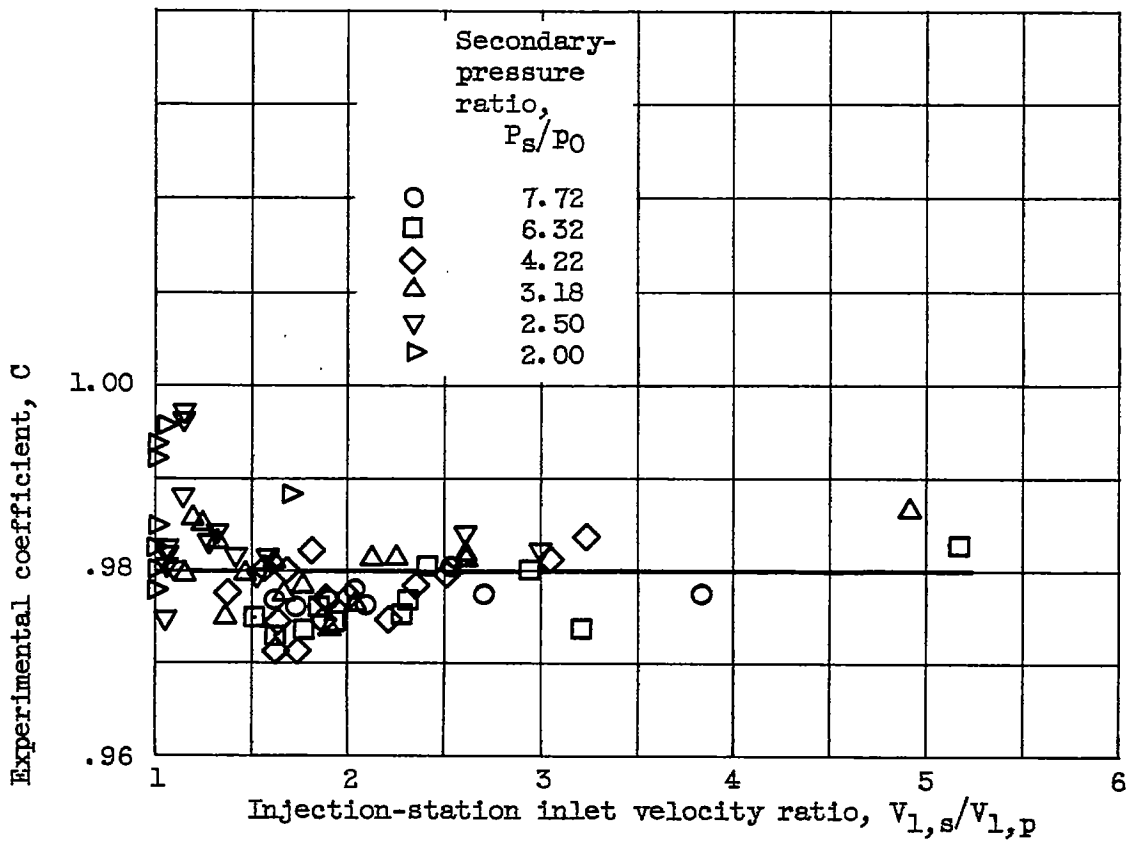

Figure 11. - Evaluation of experimental coefficient, C for all slot widths. $T_s \cong T_p \cong 530^\circ$ R.

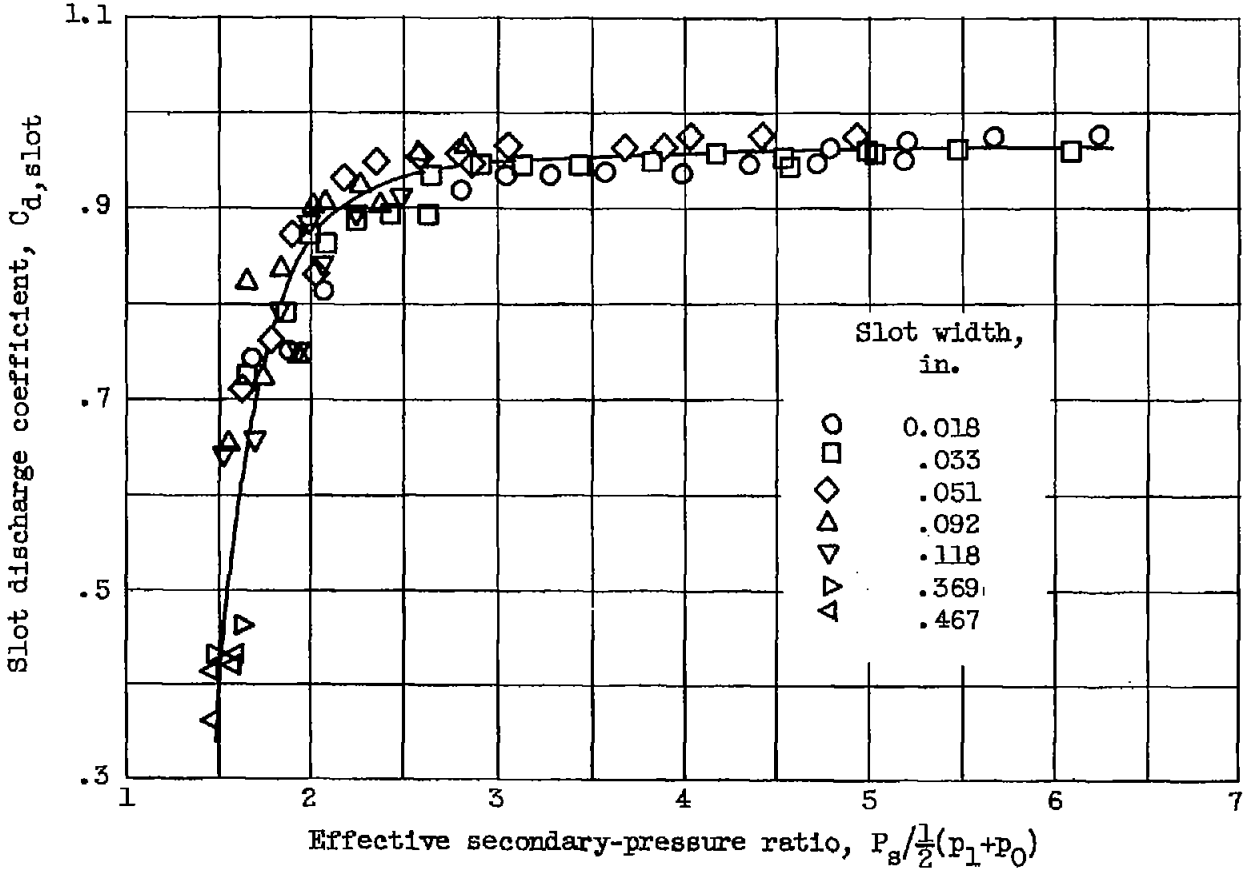

Figure 12. - Evaluation of slot discharge coefficient. $T_s \approx T_p \approx 530^\circ$ R; $1.6 \leq P_p/p_0 \leq 2.8$; $2.0 \leq P_s/p_0 \leq 7.72$.

4829

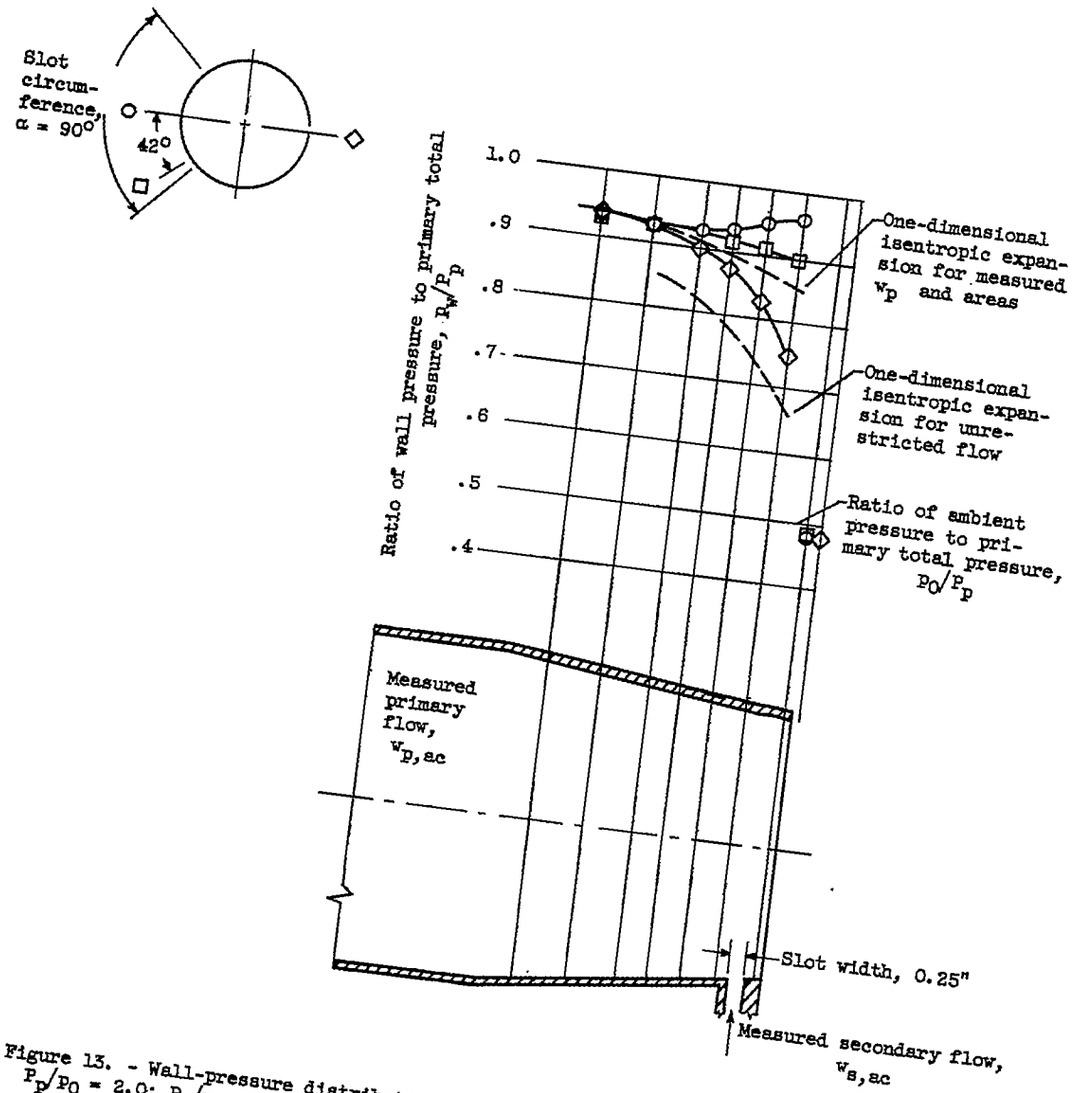

Figure 13. - Wall-pressure distribution in nozzle operated as jet deflector. $P_p/P_0 = 2.0$; $P_s/P_0 = 3.25$; $w_{s,ac}/w_{p,ac} = 0.111$; $A_{eff}/A_{eff,o} = 0.785$; side-force ratio = 0.15.

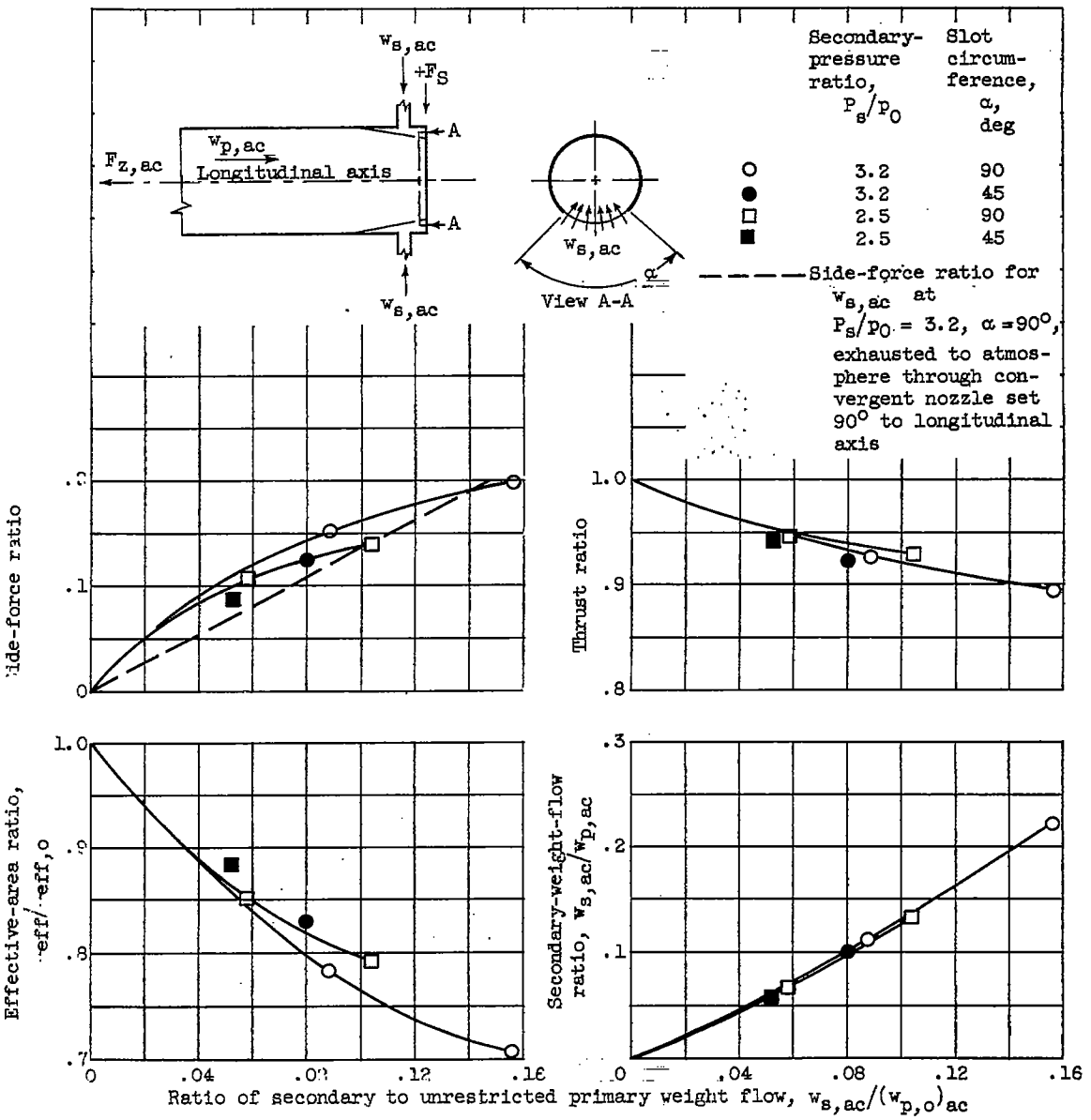

(a) Primary-pressure ratio, 2.0.

Figure 14. - Performance of nozzle operated as jet deflector. $T_s \cong T_p \cong 530°$ R.

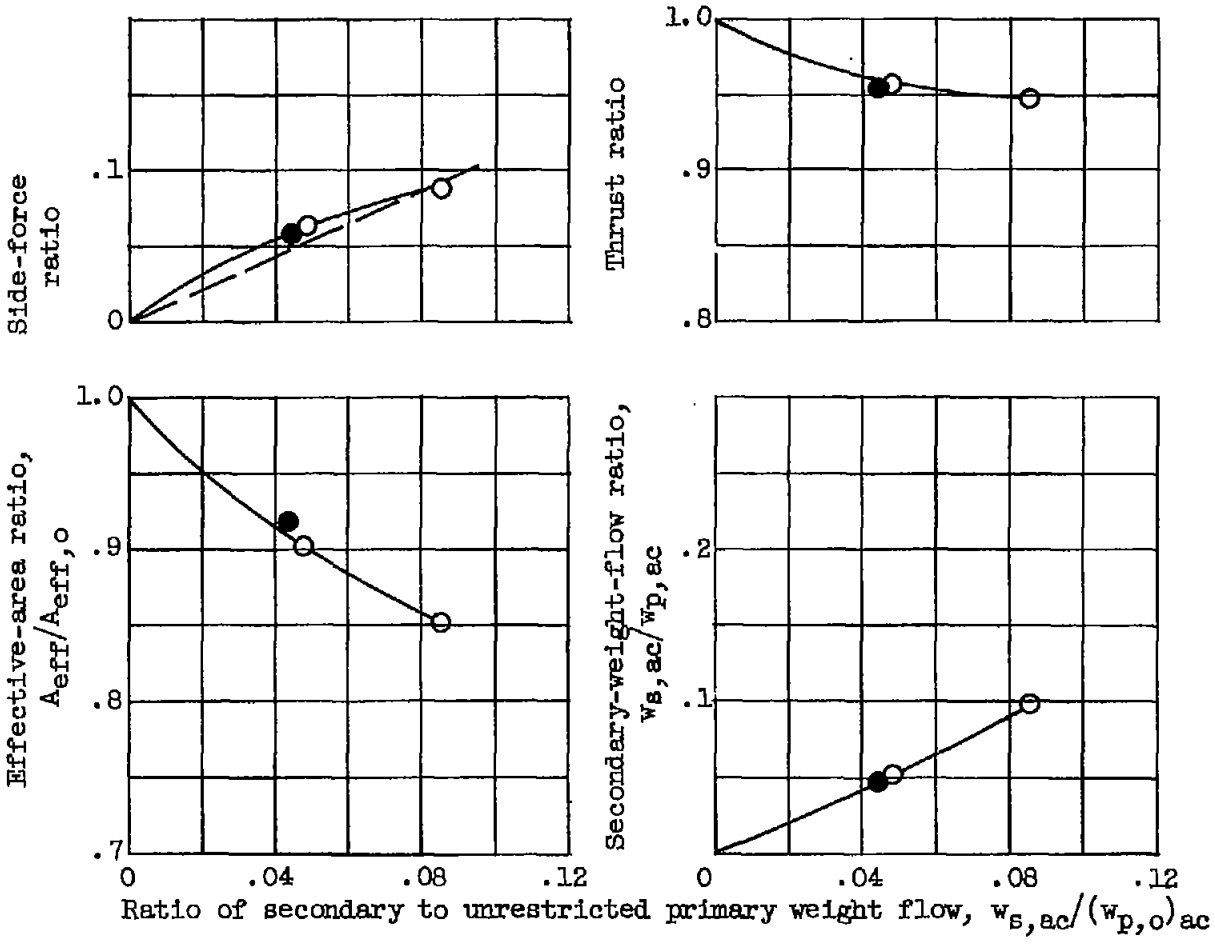

(b) Primary-pressure ratio, 2.8.

Figure 14. - Concluded. Performance of nozzle operated as jet deflector. $T_s \approx T_p \approx 530^{\circ}$ R.